

Quantum critical point in the Kondo-H eisenberg model on the honeycomb lattice

Saeed Saremi and Patrick A. Lee

Department of Physics, Massachusetts Institute of Technology, Cambridge, Massachusetts 02139

(Dated: October 10, 2006)

We study the Kondo-H eisenberg model on the honeycomb lattice at half-filling. Due to the vanishing of the density of states at the Fermi level, the Kondo insulator disappears at a finite Kondo coupling even in the absence of the Heisenberg exchange. We adopt a large- N formulation of this model and use the renormalization group machinery to study systematically the second order phase transition of the Kondo insulator (KI) to the algebraic spin liquid (ASL). We note that neither phase breaks any physical symmetry, so that the transition is not described by the standard Ginzburg-Landau-Wilson critical point. We find a stable Lorentz-invariant fixed point that controls this second order phase transition. We calculate the exponent of the diverging length scale near the transition. The quasi-particle weight of the conduction electron vanishes at this KI-ASL fixed point, indicating non-Fermi liquid behavior. The algebraic decay exponent of the staggered spin correlation is calculated at the fixed point and in the ASL phase. We find a jump in this exponent at the transition point.

I. INTRODUCTION

The interplay between charge and spin degrees of freedom has been a focus of research in complex materials such as cuprates and heavy-fermions.¹ The clearest example of this interplay is the quantum critical point seen in many heavy-fermion materials. At zero temperature, the heavy Fermi liquid (HFL) phase disappears exactly at a point where the anti-ferromagnetic (AF) magnetic ordering grows. Non-Fermi liquid behaviors are seen in the quantum critical region, i.e. the V-shaped region above this critical point.¹ The theoretical understanding of why these two seemingly different phases, i.e. AF ordered and heavy fermi liquid, should collapse at one point and a clear understanding of the non-Fermi liquid behaviors in the quantum critical region are poor at the moment.

It is by now understood that the spin density wave approach to understand the quantum critical point in heavy-fermions, known as the Moriya-Hertz-Millis theory², only accounts for small deviations from Fermi liquid theory. New theoretical approaches for understanding the quantum critical heavy-fermions are needed.

In an attempt to find an alternative for the Moriya-Hertz-Millis theory, Senthil et al. proposed recently that the AF-HFL transition might be controlled by an unstable spin liquid fixed point.^{3,4} This picture is very similar to the Deconfined quantum critical point in the context of the second order phase transition between Neel and valence bond solid (VBS) ground states.⁵ In that case the transition to VBS happens due to the existence of an unstable spin liquid on the magnetically disordered side of the critical point. Deconfined quantum critical points open up the possibility of second order phase transitions between "unrelated" phases like AF and HFL. It also has the advantage of giving a plausible scenario for the non-Fermi liquid behavior seen in experiments in heavy fermion materials. This view has had some successes in explaining some of the experimental observations.^{6,7} In this paper, we further explore this point of view.

In search for a microscopic model that provides this type of quantum critical point, we study the Kondo-H eisenberg model on the honeycomb lattice at half-filling. The heavy fermion quantum critical point in this model is simplified. It corresponds to a point, where both charge gap and spin gap vanishes. This model is given by the following Hamiltonian ($J_K > 0; J_H > 0$):

$$\hat{H} = \sum_{\langle ij \rangle, a} t_{ij;a} c_i^{a\dagger} c_j^a + H_{\text{sc}} + \sum_i J_K s_i \cdot \sum_{\langle ij \rangle} J_H S_i \cdot S_j; \quad (1)$$

where i and j live on the honeycomb lattice sites and a is the spin index: $f; \#g$. The s_i and S_i denote the conduction electron spin and the localized spin at the site i respectively. What makes the honeycomb lattice very interesting to study is the fact that the Kondo gap vanishes at a finite coupling constant even as $J_H \rightarrow 0$. This is due to the fact that, in contrast to the square lattice, the density of states of the conduction electrons vanishes at the Fermi level.⁸

The Kondo-H eisenberg model on the honeycomb lattice at half-filling is also interesting, because it can be studied by quantum Monte Carlo without the fermion sign problem.^{9,10} The present paper can be considered a prelude to such a study. In this connection we mention the quantum Monte Carlo study of the Kondo lattice model ($J_H = 0$) on the square lattice by Aissaad.¹⁰ He found a quantum phase transition of the AF ordered ground state to a disordered one caused by the Kondo exchange. The quasi-particle gap however did not vanish at the transition point,²⁶ i.e. the magnetic transition happened inside the KI phase. This made the transition a magnetic transition belonging to the $O(3)$ nonlinear sigma model universality class. Note that the nested Fermi line of the tight-binding band provides the instability towards AF at $(\pi; \pi)$ even in the absence of the Heisenberg exchange J_H . In contrast the honeycomb lattice tight binding band has Fermi points in the corner of the Brillouin zone called the Dirac points. This causes the nesting to be extremely weak as compared to the per-

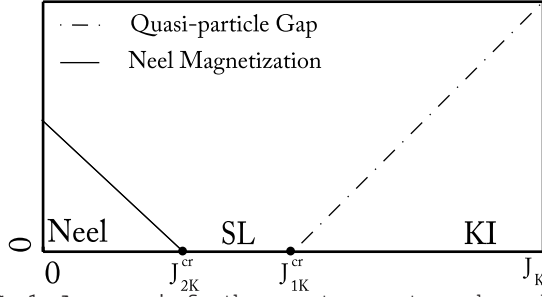


FIG. 1: A scenario for the zero temperature phase diagram of the Kondo-Hamiltonian on the honeycomb lattice at half-filling [given by Hamiltonian Eq. (1)] as a function of J_K ($t = 1$) for a sufficiently small J_H . In contrast to the same model on a square lattice, Kondo gap denoted schematically by the dotted-dashed line vanishes at a finite coupling constant J_{1K}^{cr} . The weak nesting of the Dirac nodes of the honeycomb lattice makes the KI transition to a spin liquid ground state plausible.

fectly nested lines of the Fermi line in the square lattice.

Next we consider different scenarios for the ground state phase diagram of our model, where we consider varying J_K ($t = 1$), keeping J_H to be small. In the limit $J_K \rightarrow J_H$, the Heisenberg exchange dominates and will lead to Neel ordering with opposite spins on the AB sublattices of the honeycomb lattice.

In the first scenario, sketched schematically in Fig. 1, the finite coupling Kondo transition is to a magnetically disordered ground state (spin liquid). In this scenario the AF ordered ground state does not survive up to the KI transition point for sufficiently small J_H . The Kondo physics has stabilized a spin liquid ground state in the region between the KI and AF ground states. The charge gap closes at J_{1K}^{cr} , as the KI gives way to a semimetal. The spin gap may or may not be finite, depending on the nature of the spin liquid. As J_K is further reduced a transition to the Neel phase occurs. This scenario will of course be very exciting, if a spin liquid can indeed be stabilized as the ground state over some parameter range.

The other exciting possibility is that a continuous transition between two distinct orders (AF and KI) exists over a finite parameter range. This scenario is sketched schematically in Fig. 2. In this scenario SL is unstable to Neel ordering. This will be an example of the deconfined quantum critical point mentioned earlier. Finally, scenarios in which an overlapping region, where a Neel state coexists with the Kondo insulator (similar to the square lattice result of Assaad¹⁰); or a first order transition can not be ruled out. With these motivations we now sketch an outline of this paper.

In this paper we begin by a mean-field study of the Kondo-Hamiltonian model Eq. (1) on the honeycomb lattice. We adopt a fermionic representation for localized spins. We make a mean-field decoupling of $S_i^\alpha S_j^\beta$ in the fermionic hopping channel. This is sometimes referred to as the resonating valence bond (RVB) decoupling. The Kondo interaction is decoupled in the usual mean-field way with the hybridization order parameter

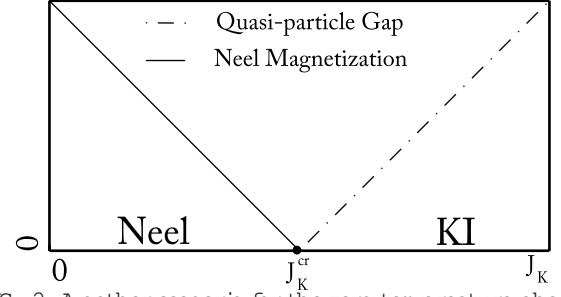


FIG. 2: A another scenario for the zero-temperature phase diagram for the Kondo-Hamiltonian at half-filling on the honeycomb lattice for some (maybe "tuned") Heisenberg exchange J_H as a function of J_K . In contrast to the same model on a square lattice, both the quasi-particle gap denoted schematically by the dotted-dashed line and Neel order parameter denoted by the solid line vanishes at $J_K = J_K^{cr}$.

$b = \frac{D_P}{f_1^{ay} c_1^a} E$. The nonzero b will correspond to the KI phase, where the gap in the dispersion is proportional to b . For any $J_H > 0$ we find a continuous transition between the KI ($b \neq 0$) and a spin liquid state (see Fig. 3). This spin liquid is characterized by Dirac fermions coupled to $U(1)$ gauge field, and has been called the algebraic spin liquid (ASL), because the spin correlation decays as a power law and spin excitations are gapless.¹²

As mentioned earlier, in the $J_K \rightarrow J_H$ limit, localized spins will be Neel ordered. Our mean-field decoupling can not capture this.²⁷ Here we proceed with the assumption that the phase diagram is given by Fig. 1 and our main interest is to study the KI to SL transition. For this purpose the RVB decoupling is a reasonable starting point.

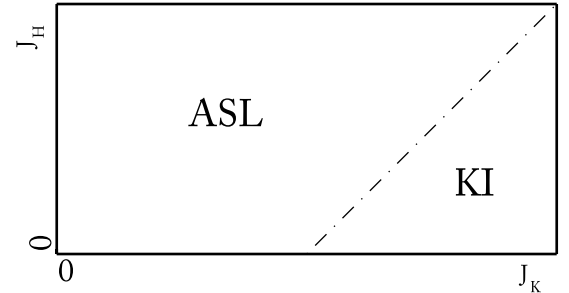


FIG. 3: The mean-field phase diagram of the Hamiltonian given by Eq. (1) in the $J_K - J_H$ space ($t = 1$). For any $J_H > 0$, we find a transition from the KI to the algebraic spin liquid.

The rest of the paper is devoted to studying the critical properties of the fixed point that controls the transition from the KI to ASL. We note that neither phase breaks any physical symmetry, so that the transition is not described by the standard Ginzburg-Landau-Wilson critical point. What changes at the transition is the dynamics of an emergent gauge field. The emergent gauge field is confined in the KI phase and it is deconfined in the ASL phase.

In Sec. IIB we generalize our model by letting the spin indices to run from 1 to N rather than just "up" and "down". The saddlepoint approximation (i.e. the mean-

eld) becomes exact as $N \rightarrow 1$. In Sec. III we derive the low-energy Lagrangian density which sets the stage for a systematic $1/N$ expansion.

Section IV develops the propagator for the Kondo eld b , and the gauge eld a in the leading order. The Kondo eld propagator can be tuned to a massless point at $J_K = J_K^{cr}$. In the $J > J_K^{cr}$ regime the b eld condenses to $\langle b \rangle$ and we will be in the Higgs phase where the gauge eld is massive. This is nothing but the Kondo physics, where the excitation gap is proportional to $\langle b \rangle$. In the $J < J_K^{cr}$ regime the Kondo eld is not condensed, and is massless. The physics is described by Dirac fermions coupled to a $U(1)$ gauge eld. This eld theory, known as QED_3 , has been studied extensively^{12,16}, and is understood to be an algebraic spin liquid due to algebraic correlation of spins.¹² This phase is believed to be deconfined.¹³

Section V A contains the main technical calculation of this paper. We calculate the exponent ν , which describes the diverging length scale of the transition. We consider a relativistic fixed point, which allows us to adopt standard eld theory methods. In Sec. V B we calculate the decay exponent of the staggered localized spin. In Sec. V I we show that the relativistic fixed point is stable and is therefore the appropriate fixed point to study for the transition.

II. FINITE COUPLING KONDO TRANSITION

A. Mean-Field Transition

Our starting point is the Hamiltonian

$$\hat{H} = \sum_{\langle ij \rangle, a} t_{ij,a} c_i^{ay} c_j^a + H_{sc} + \sum_i J_K s_i \cdot \hat{S}_i + \sum_{\langle ij \rangle} J_H s_i \cdot s_j \quad (2)$$

where i and j live on the honeycomb lattice sites and a is the spin index: $f; \uparrow; \downarrow$. The s_i denotes the conduction electron spin at the site i and the capital S_i denotes the localized spin at the site i and they both are $SU(2)$ spins with an $SU(2)$ spin algebra. The conduction electron spin is given by

$$s_i = \frac{1}{2} c_i^{ay} c_{i,ab}^b; \quad (3)$$

where $\sigma = (x; y; z)$ are the Pauli matrices. We adopt a fermionic representation for localized spins, where their Hilbert space $f \uparrow_i; \uparrow_i g$, is constructed using Fermionic operators:

$$\begin{aligned} \uparrow_i &= f_i^{\uparrow y} \downarrow_i; \\ \downarrow_i &= f_i^{\uparrow y} \downarrow_i; \end{aligned} \quad (4)$$

The anti-commutation relation:

$$f_i^{ay} f_j^b = -\delta_{ab} \delta_{ij} \quad (5)$$

together with

$$S_i = \frac{1}{2} f_i^{ay} c_{i,ab}^b \quad (6)$$

will result in the $SU(2)$ commutation relations for spin S . However, the Hilbert space of the localized spin S_i is restricted to only two elements: $f \uparrow_i; \uparrow_i g$. Therefore identifying localized spin by fermionic operators given by Eq. (6) has to be accompanied by the constraint

$$\sum_a f_i^{ay} f_i^a = 1; \quad (7)$$

Combining Eqs. (3) | (7); together with the following identity for the Pauli matrices

$$a_b c_d = 2 \delta_{ad} b_c - a_b c_d \quad (8)$$

one finds a fermionic representation of the spin-spin interactions in the Hamiltonian of Eq. (2):

$$s_i \cdot s_j = \frac{1}{4} \sum_a c_i^{ay} c_j^a - f_i^{by} c_j^b + H_{sc} + \frac{1}{4}; \quad (9)$$

$$S_i \cdot S_j = \frac{1}{4} \sum_a f_i^{ay} f_j^a - f_j^{by} f_i^b + H_{sc} + \frac{1}{4}; \quad (10)$$

where the sum over the spin indices is understood.

The four-fermion interaction terms of Eqs. 9 and 10 will be replaced in the mean-eld (MF) simplification by a quadratic interaction:

$$\hat{A} = \hat{A}_1 \hat{A}_2 + h_{A_1 i} \hat{A}_2 + \hat{A}_1 h_{A_2 i} - h_{A_1 i} h_{A_2 i}; \quad (11)$$

where \hat{A} denotes a generic four-fermion interaction term. To make the interaction quadratic one has to ignore $(\hat{A}_1 h_{A_2 i}) (\hat{A}_2 - h_{A_2 i})$. So the mean-eld parameters have to satisfy the self-consistency condition:

$$\frac{\partial F_{MF}}{\partial h_{A_1 i}} = \frac{\partial F_{MF}}{\partial h_{A_2 i}} = 0; \quad (12)$$

We make the interaction terms given by Eqs. (9) and (10) quadratic by choosing the following mean-eld parameters:

$$\sum_a c_i^{ay} f_i^a = \langle b \rangle \uparrow_i; \quad (13)$$

$$\sum_a f_i^{ay} f_j^a = \langle b \rangle \uparrow_{ij} \uparrow_{ij}; \quad (14)$$

The first parameter $\langle b \rangle \uparrow_i$ lives on sites. The second parameter $\langle b \rangle \uparrow_{ij} \uparrow_{ij}$ lives on links. We assume that these parameters have a constant magnitude throughout the lattice. When they take a non-zero value, small deviations from their "constant" magnitudes cost energy: they are locally stable. $\langle b \rangle = 0$ corresponds to the Kondo insulator phase, where the gap in the excitations is proportional to $\langle b \rangle$. We also note that the conventional decoupling of $S_i \cdot S_j$ leads to the anti-ferromagnetic order

parameter $\hbar S_{iz}$. In this paper we adopt the alternative decoupling of Eq. (14), which is often called the RVB (Resonating Valence Bond) decoupling. RVB decoupling leads to a spin liquid state.

The U(1) gauge freedom in defining f gives the freedom to eliminate a_i by the following gauge transformation:

$$\begin{aligned} f_i^a &\rightarrow e^{i\phi_i} f_i^a; \\ a_{ij} &\rightarrow a_{ij} + (\phi_i - \phi_j); \end{aligned} \quad (15)$$

This transformation leaves the total flux modulo 2

$$\sum_{ij \in \text{hexagon}} a_{ij} \pmod{2} \quad (16)$$

through any closed loop invariant. Next we make a choice $\phi_{ij} = \phi_i - \phi_j$ where ϕ_i is real. This choice corresponds to the case where the total flux through each hexagon modulo 2 is zero.

Our mean-field choices result in the following mean-field Hamiltonian:

$$\begin{aligned} \hat{H}_{MF} = & \sum_i t \sum_{\langle ij \rangle} c_i^{ay} c_j^a + H.c. \\ & + \frac{J_K}{2} \sum_i b_i^X f_i^{ay} c_i^a + H.c. \\ & + \frac{J_H}{2} \sum_i f_i^{ay} f_j^a + H.c. \\ & + N \left(J_K b^2 + \frac{3J_H}{2} \right); \end{aligned} \quad (17)$$

where N is the number of unit cells. The different coefficients of the constant terms are due to the fact that there are 2 sites as opposed to 3 links per unit cell. We also mention that, at the mean-field level, the constraint given by Eq. (7) is enforced on average by having a chemical potential for f fermions. This chemical potential is zero due to f -fermions particle-hole symmetry.

From \hat{H}_{MF} , the MF free energy can be calculated numerically. MF parameters satisfying the self-consistency condition are then obtained. The numerics confirm the finite coupling Kondo transition in a background ν , for any $J_H > 0$. Next we show this finite coupling Kondo transition analytically and find the exponent

$$\nu = \frac{1}{2} \left(\frac{J_K}{J_H} \right)^{2/3}; \quad (18)$$

by focusing on the low-energy theory near the Dirac nodes.

We focus first on the conduction electrons kinetic term $\sum_i t \sum_{\langle ij \rangle} c_i^{ay} c_j^a + H.c.$. We do the Fourier transformation

$$c_A(\mathbf{k}) = \frac{1}{N} \sum_{\mathbf{R}} e^{i\mathbf{k} \cdot \mathbf{R}} c_A(\mathbf{R}) \quad (19)$$

where \mathbf{R} are the Bravais lattice vectors and $c_A(\mathbf{R})$ is the conduction electron annihilation operator at the A sublattice site of the unit cell positioned at \mathbf{R} . The similar transformation is done to get $c_B(\mathbf{k})$. Conduction

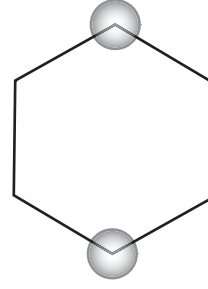


FIG. 4: The Brillouin zone of the honeycomb lattice. Corners of the Brillouin zone are where the tight-binding gap vanishes. The independent low-energy modes are denoted by the filled circles around the two Dirac nodes \mathbf{k}_D .

electrons kinetic term in momentum space will take the form:

$$\sum_{ij} t_{ij}^y c_j + H.c. = \sum_{\mathbf{k}} t(\mathbf{k}) c_A^y(\mathbf{k}) c_B(\mathbf{k}) + H.c.; \quad (20)$$

where

$$t(\mathbf{k}) = 1 + e^{ik_x(2a_1 - a_2)} + e^{ik_x(2a_1 + a_2)}; \quad (21)$$

and $\mathbf{a}_1 = a(1; 0)$ and $\mathbf{a}_2 = a(-1/2; \sqrt{3}/2)$ are two of the three vectors that connect A sublattice sites to nearest neighbor B sublattice sites. a is the length between nearest neighbor sites which will be set to the unit length: $a = 1$.

$t(\mathbf{k})$ vanishes at the Dirac nodes \mathbf{k}_D , which is given by

$$\mathbf{k}_D = 0; \pm \frac{4\pi}{3} \hat{y}; \quad (22)$$

Near the nodes as schematically represented by the filled circles in the Fig. 4, $t(\mathbf{k}_D + \mathbf{q})$ is given by

$$t(\mathbf{k}_D + \mathbf{q}) = \frac{3}{2} (iq_1 - q_2) + O(q^2); \quad (23)$$

To write the conduction electron kinetic term near the Dirac nodes, we use the following notation, which will also be helpful in Sec. III:

$$c(\mathbf{q}) = \begin{pmatrix} c_A(\mathbf{k}_D + \mathbf{q}) \\ c_B(\mathbf{k}_D + \mathbf{q}) \end{pmatrix}; \quad (24)$$

After collecting Eqs. (20) – (24), we get

$$\begin{aligned} \sum_{ij} t_{ij}^y c_j + H.c. = & \sum_{\mathbf{q}} \frac{3t}{2} c(\mathbf{q})^\dagger \begin{pmatrix} q_1 - 2q_2 \\ q_1 - q_2 \end{pmatrix} c(\mathbf{q}) \\ & + \sum_{\mathbf{q}} \frac{3t}{2} c(\mathbf{q})^\dagger \begin{pmatrix} q_1 - 2q_2 \\ q_1 - q_2 \end{pmatrix} c(\mathbf{q}); \end{aligned} \quad (25)$$

where \mathbf{q} is used, since in contrast to Eq. (20) the momentum sum is restricted to be near the Dirac nodes.

Next we obtain the energy dispersion near the node $+k_D$. The M F Hamiltonian in momentum space and near the node $+k_D$, denoted by $\hat{H}_+(q)$, is given by

$$\hat{H}_+(q) = \begin{pmatrix} v_c & 0 \\ 0 & v_f \end{pmatrix} + \begin{pmatrix} 0 & J_K b \\ J_K b & 0 \end{pmatrix} ; \quad (26)$$

where we have dropped the constant term of Eq. (17) and we have used a similar notation as in Eq. (24) for the fermions:

$$\begin{pmatrix} f_A \\ f_B \end{pmatrix} = \begin{pmatrix} f_A(k_D + q) \\ f_B(k_D + q) \end{pmatrix} ; \quad (27)$$

The 4 × 4 matrix H_+ is given in block form by

$$H_+ = \frac{1}{2} \begin{pmatrix} 2v_c(q_{\parallel 2} + q_{\perp 1}) & J_K b \\ J_K b & 2v_f(q_{\parallel 2} + q_{\perp 1}) \end{pmatrix} ; \quad (28)$$

where v_c and v_f are given by:

$$v_c = \frac{3}{2}t; \quad (29)$$

$$v_f = \frac{3}{4}J_H ; \quad (30)$$

It will be clear why notations v_c and v_f is used shortly. It is straightforward to diagonalize the above matrix. The four eigenvalues are given by:

$$e(q) = \begin{pmatrix} v_c & v_f \end{pmatrix} \pm \sqrt{(v_f + v_c)^2 q^2 + J_K^2 b^2} = 2; \quad (31)$$

We have dropped the subscript $+$ from $e(q)$, since the dispersion near the other node is the same.

To understand the above dispersion better, we mention its behavior in different regimes:

$b = 0$. The M F Hamiltonian has two decoupled parts: kinetic terms for the conduction electrons and for fermions. In this case the 4 eigenvalues near the nodes become $v_c \pm q$ and $v_f \pm q$. They are the massless Dirac dispersions for conduction electrons and fermions with velocities v_c and v_f respectively. The phase with $b = 0$ is an algebraic spin liquid phase as will be clear in Sec. V B. This is closely related to the work of Rantner and Wen, where Dirac fermions coupled to a gauge field was found to be an algebraic spin liquid.¹²

$v_f = v_c, b \neq 0$. The dispersion is the massive relativistic Dirac dispersion

$$e(q) = \sqrt{v_c^2 q^2 + (J_K b)^2}; \quad (32)$$

where each eigenvalue is doubly degenerate. $J_K b = 2$ is the mass of our relativistic quasi-particles. In Sec. III, we will see that the low-energy theory, in the limit $v_f = v_c$, is Lorentz invariant. The above relativistic dispersion is a sign of this Lorentz invariance.

sign of v_f . The sign of (v_f) has dramatic consequences on the shape of the dispersion and also on the continuum formulation of the model near the phase transition. Due to the coupling between fermions and the conduction electrons the free energy is not invariant under the mapping $v_f \rightarrow -v_f$. In the Kondo insulating phase ($b \neq 0$); the dispersion for $v_f > 0$ is gapped. However the dispersion for $v_f < 0$ has a gapless ring around each Dirac node with the radius

$$q_c = \frac{J_K b}{2\sqrt{v_f}} ; \quad (33)$$

It turns out that the positive (self consistent) ($v_f > 0$) is more stable. This is not surprising from the above fact that the dispersion for $v_f > 0$ is gapped as opposed to $v_f < 0$ which is gapless. We are only concerned with the stable solution $v_f > 0$ in this paper.

The M F transition at zero temperature can be analyzed by minimizing the total energy

$$E = 4 \sum_{e(q) < 0} e(q) + N \left[J_K b^2 + \frac{3J_H}{2} b^2 \right] ; \quad (34)$$

$$\frac{\partial E}{\partial b} = 0; \text{ and } \frac{\partial E}{\partial v_f} = 0; \quad (35)$$

The coefficient $4 = 2 \times 2$ is for counting spins and the two nodes. The condition $\frac{\partial E}{\partial b} = 0$ at $b = 0$ results in the self consistent v_f , which varies slowly across the transition. For $v_f > 0$, the negative energy bands are given by

$$\begin{pmatrix} v_c & v_f \end{pmatrix} \pm \sqrt{(v_f + v_c)^2 q^2 + J_K^2 b^2} = 2. \text{ Therefore} \\ \sum_{e(q) < 0} e(q) = \sum_q \sqrt{(v_f + v_c)^2 q^2 + J_K^2 b^2}; \quad (36)$$

Combine Eqs. 34 | 36, to arrive at the self-consistency equation for b :

$$\frac{2}{N} \sum_q \sqrt{(v_f + v_c)^2 q^2 + J_K^2 b^2} = 1; \quad (37)$$

It is clear from the above equation that the Kondo phase does not survive down to $J_K = 0$, in contrast to the case when the conduction band possess a Fermi surface. The Kondo insulator phase disappears at a finite coupling constant J_K^{cr} . Taking the limit $N \rightarrow 1$, we find the following dependence of the Kondo parameter b as a function of the distance from the transition $J_K - J_K^{cr}$:

$$b \propto (J_K - J_K^{cr})^{1/2}; \\ J_K^{cr} = \frac{v_c + v_f}{2}; \quad (38)$$

where 1 is a large-momentum cutoff around the Dirac nodes k_D .

To summarize, the M F solution has two interesting features:

The Kondo insulator phase disappears at a finite coupling constant.

The Kondo condensate $\langle b_j \rangle$ vanishes linearly as the distance from the critical point. We emphasize that a Landau-type expansion for the b mean-field parameter would yield the result $\langle b_j \rangle / (J_K - J_K^c)^{1/2}$ near the transition point. The appearance of non-trivial critical exponent at the mean-field level is characteristic of the coupling of b to gapless fermions which is addressed systematically in the $1/N$ expansion.

B. Large N Formulation : Mean-Field Justified

In this section we extend the physical model with two spin- flavors to a generalized model with N spin- flavors.¹¹ We show that the mean-field solution is the stable solution in the infinite N limit.

The conduction electrons kinetic term $\sum_i c_i^{ay} c_j^a + H.c.$ is already in the generalized form. We just let the spin index a to run from 1 to N. The spin-spin interactions as written in Eqs. 9 and 10 is also easily generalized by letting the spin indices to run from 1 to N. In addition we control these interactions by replacing $\frac{1}{2}$ with $\frac{1}{N}$. So the generalized version of the Hamiltonian of Eq. (2) is given by

$$\hat{H} = \sum_i \sum_{a,b} c_i^{ay} c_j^a + H.c. + \frac{J_K}{2N} \sum_{\langle ij \rangle} \sum_a (f_i^{ay} f_j^a) (f_i^{by} f_j^b) + H.c. + \frac{J_H}{2N} \sum_{\langle ij \rangle} \sum_a (f_i^{ay} f_j^a) (f_j^{by} f_i^b) + H.c. ; \quad (39)$$

where the sum over spin indices is understood. The above Hamiltonian has to be accompanied by the local constraint:

$$\sum_a f_i^{ay} f_i^a = \frac{N}{2} ; \quad (40)$$

The above generalized model will coincide with the Hamiltonian Eq. (2) for $N=2$. In fermion coherent state representation, using Grassmann variables, the Euclidean Lagrangian and the partition function take the form

$$L_E(c; f; a_0) = \sum_i c_i^a(x_0) \partial_0 c_i^a(x_0) + f_i^a(x_0) \partial_0 f_i^a(x_0) + i a_0 \sum_i f_i^a(x_0) f_i^a(x_0) - \frac{N}{2} + H ; \quad (41)$$

$$Z = \int D[c f f a_0] e^{\int dx_0 L_E(x_0)} ;$$

where x_0 denotes the imaginary time. The field a_{i0} , when integrated over, will produce delta functions at each site enforcing the local constraint given by Eq. 40. The notation a_{i0} is used because it will serve as the time component of the emergent gauge field.

Next we do the standard Hubbard-Stratonovich transformation to decouple the four-fermion terms in the action at a cost of introducing the complex fields b_i , which live on sites and ij , which live on links:

$$L_E(c; f; b; a_0) = \sum_i c_i^a \partial_0 c_i^a + \sum_{\langle ij \rangle} t_{ij} c_i^a c_j^a + H.c. + \sum_i f_i^a (\partial_0 - i a_{i0}) f_i^a + i N a_{i0} = 2 + \sum_{\langle ij \rangle} \frac{N}{J_H} j_{ij} f_j^2 + j_{ij} f_i^a f_j^a + j_{ij} f_j^a f_i^a + \sum_{\langle ij \rangle} \frac{N}{J_K} b_{ij} f_j^2 + b_i c_i^a f_i^a + b_i f_i^a c_i^a ; \quad (42)$$

$$Z = \int D[c f f b a_0] e^{\int dx_0 L_E(x_0)} ;$$

The x_0 dependence of Grassmann and complex fields in the Lagrangian is understood as well as the dropped indices in the measure of the path integral.

The action is quadratic in the fermionic fields and it can be integrated out at the cost of obtaining an effective action for b_i and ij fields, which is highly nonlocal. Since there is no mixing of different spin- flavors, the resulting effective action will be proportional to N :

$$\frac{L_E(b; j)}{N} = \log \det M + \frac{1}{J_K} \sum_i b_i f_i^2 + \frac{1}{J_H} \sum_{\langle ij \rangle} j_{ij} f_j^2 ; \quad (43)$$

M is a $4N \times 4N$ Hermitian matrix, which encodes the quadratic interaction of the fermionic fields as given by Eq. (42), e.g. $M_{c_i f_i} = b_i$.²² The $\log \det M$ makes the effective Lagrangian in terms of b_i and ij fields nonlocal.

The saddle point approximation for the above Lagrangian $L_E(b; j)$ is exact as $N \rightarrow \infty$. The saddle point equations will be the mean-field equations given by Eq. (12), and this is how the mean-field developed in the previous section is justified. Furthermore the Lagrangian given in Eq. (42) will set the stage for a systematic $1/N$ expansion around the mean-field solution.

III. BEYOND MEAN-FIELD : LOW-ENERGY EFFECTIVE FIELD THEORY

In this section we obtain the Lagrangian density near the critical point starting from the microscopic Lagrangian. There are two independent nodes k_y and

near each node there are fermions from A and B sublattices. We package these c and f fermions into four component spinors. This is done in a way to make the kinetic terms for both fields look the same.

Since there is no mixing of different spin- flavors in the microscopic Lagrangian Eq. (42), we will drop this index throughout the derivation of the Lagrangian density. The spin- flavor index will be resurrected at the end.

The kinetic term for the conduction electrons was discussed in Sec. IIA :

$$\begin{aligned} \sum_{\mathbf{r}} \bar{c}_{\mathbf{r}}^{\dagger} c_{\mathbf{r}} + H.c. = & \sum_{\mathbf{r}} \bar{\psi}_{\mathbf{r}}^{\dagger} + (q)^{\dagger} (q_{\mathbf{r}+2} + q_{\mathbf{r}-1}) + (q) \\ & + v_c \sum_{\mathbf{r}} (q)^{\dagger} (q_{\mathbf{r}+2} - q_{\mathbf{r}-1}) + (q) \end{aligned} \quad (44)$$

Note that under the transformation $(q) \rightarrow (q)^\dagger$ the second term has the same form as the first one. We combine the two 2-component spinors, associated with the two Dirac nodes, to form a 4-component spinor (q) :

$$(q) = \begin{pmatrix} (q) \\ (q)^\dagger \end{pmatrix} \quad (45)$$

To write the kinetic term in terms of (q) , we define the 4x4 block diagonal matrices γ_i :

$$\gamma_i = \begin{pmatrix} 0 & 1 \\ 1 & 0 \end{pmatrix} = \gamma_i \gamma_2 \gamma_3 \quad (46)$$

The kinetic term then takes the form

$$\sum_{\mathbf{r}} \bar{c}_{\mathbf{r}}^{\dagger} c_{\mathbf{r}} + H.c. = \sum_{\mathbf{r}} \bar{\psi}_{\mathbf{r}}^{\dagger} (q)^{\dagger} (q_{\mathbf{r}+2} + q_{\mathbf{r}-1}) + (q) \quad (47)$$

After taking the continuum limit, the Lagrangian density corresponding to this Hamiltonian is:

$$L_E^{(1)} = \bar{\psi} \gamma_0 \partial_t \psi + v_c \bar{\psi} \gamma_2 (\partial_1 \psi + \partial_1 \bar{\psi}) \quad (48)$$

To use the field theory techniques one would write $L_E^{(1)}$ in a different form

$$L_E^{(1)} = \bar{\psi} \gamma_0 \partial_t \psi + v_c \bar{\psi} (\partial_1 \psi + \partial_1 \bar{\psi}) \quad (49)$$

where ψ is defined to be

$$\psi = \begin{pmatrix} \psi \\ \psi^\dagger \end{pmatrix} \quad (50)$$

Next we focus on $\sum_{ij} f_i^{\dagger} f_j^{\dagger} + \sum_{ij} f_j^{\dagger} f_i^{\dagger}$ term in Eq. (42). Consider the mean-field case $\langle f_{ij} \rangle = \langle f_{ji} \rangle > 0$. The phase fluctuations will be included as gauge field fluctuations later on. Ignoring the phase fluctuations, this term looks exactly like the kinetic term of the conduction electrons given by Eq. (44), but with an opposite sign:

$$\begin{aligned} \sum_{\mathbf{r}} \bar{f}_{\mathbf{r}}^{\dagger} f_{\mathbf{r}} + H.c. = & \sum_{\mathbf{r}} \bar{\psi}_{\mathbf{r}}^{\dagger} + (q)^{\dagger} (q_{\mathbf{r}+2} - q_{\mathbf{r}-1}) + (q) \\ & + v_f \sum_{\mathbf{r}} (q)^{\dagger} (q_{\mathbf{r}+2} - q_{\mathbf{r}-1}) + (q) \end{aligned} \quad (51)$$

We make this look like Eq. (47) by a further transformation to absorb the minus sign and we again combine the 2-component spinors near the two nodes to form a 4-component spinor (q) :

$$(q) = \begin{pmatrix} \psi \\ \psi^\dagger \end{pmatrix} \quad (52)$$

On the grounds of gauge invariance, we write the Lagrangian density corresponding to the "kinetic" term of the f fermions

$$L_E^{(2)} = \bar{\psi} \gamma_0 (\partial_0 \psi + \partial_0 \bar{\psi}) + v_f \bar{\psi} \gamma_1 (\partial_1 \psi + \partial_1 \bar{\psi}) + \bar{\psi} \gamma_2 (\partial_2 \psi + \partial_2 \bar{\psi}) \quad (53)$$

where the non-compact gauge field $a(x)$ appears as a connection to produce covariant derivative. It is related to the phase a_{ij} through the relation $a(x) = a_{ij} \hat{e}_{ij}$, where \hat{e}_{ij} is the unit vector connecting the site i to the site j . We have used the same definition as in Eq. (50):

$$\hat{e}_{ij} = \begin{pmatrix} \hat{e}_{ij} \\ \hat{e}_{ij}^\dagger \end{pmatrix} \quad (54)$$

En route to the continuum limit, we have implicitly dropped the compact character of the gauge field. This is only valid if the gauge fluctuations are not very strong. In the imaginary time evolution, there will be events on the lattice scale that change the flux of the gauge field by 2π . If these events do not proliferate, we will be in small gauge coupling constant regime and taking the continuum limit is justified.¹⁹ We return to this point at the end of this section.

Now we focus on the interaction term $\sum_i b_i c_i^{\dagger} f_i$. We write this in the momentum space and restrict c and f fermions momentum to be near k_F , and b momentum to be near $k = 0$. Simple manipulations

$$\bar{\psi} (q) + (q^0) = \bar{\psi} (q) \gamma_3 (\gamma_3 + (q^0)); \quad (55)$$

$$\bar{\psi} (q) - (q^0) = (\gamma_2 (q))^{\dagger} \gamma_3 (\gamma_1 - (q^0)); \quad (56)$$

combined with the definitions for ψ and $\bar{\psi}$ fields, result in

$$\begin{aligned} \bar{\psi} (q) + (q^0) + \bar{\psi} (q) - (q^0) &= \bar{\psi} (q) \gamma_3 (q^0) \\ &= (q) (q^0); \end{aligned} \quad (57)$$

Therefore in the continuum limit the Lagrangian density corresponding to $\sum_i b_i c_i^{\dagger} f_i + b_i f_i^{\dagger} c_i$ will be

$$L_E^{(3)} = b + b^{\dagger} \quad (58)$$

Now collect $L_E^{(1)}$, $L_E^{(2)}$ and $L_E^{(3)}$, to write the Lagrangian density

$$\begin{aligned} L_E^{v_c=v_f} = & \bar{\psi} \gamma_0 \partial_t \psi + \bar{\psi} \gamma_1 (\partial_1 \psi + \partial_1 \bar{\psi}) + \bar{\psi} \gamma_2 (\partial_2 \psi + \partial_2 \bar{\psi}) \\ & + b \bar{\psi} \psi + b^{\dagger} \bar{\psi} \psi + \frac{N}{J_K} \bar{\psi} \psi^2 + \dots \end{aligned} \quad (59)$$

where the spin indices are restored. $\bar{\psi}$ is defined to be

$$\bar{\psi} = (\bar{\psi}_1; \bar{\psi}_2); \quad (60)$$

and $\bar{\psi}$ is a shorthand for $\bar{\psi}^*$ with $\gamma = 1$. The velocity v_f in Eq. (53) is absorbed by scaling x and a . As a result, the velocities enter only as the dimensionless ratio $v_c = v_f$ via $v_c = v_f$.

Taking the continuum limit, which is essentially a coarse graining process, generates new interactions among coarse grained elds.²⁰ The ellipsis in Eq. (59) denotes such new interactions. Not all possible terms are allowed though. Since the coarse graining process does not break symmetries of the microscopic Lagrangian, the generated interactions should respect these symmetries.¹⁷

Next we set $v_f = v_c$ to make the low-energy theory Lorentz symmetric. The action in the presence of two different velocities will not respect the Lorentz symmetry. Under RG transformation in the absence of Lorentz symmetry the velocities will change, since there is no symmetry to protect them from changing. We shall show later that the Lorentz invariance is protected in the RG sense, in that small deviation from $v_f = v_c$ will scale to zero under RG transformation. Thus we focus our discussion on this Lorentz invariant fixed point.

The Lorentz-symmetric Lagrangian density is given by:

$$\begin{aligned} L_E = & \bar{\psi} \not{\partial} \psi + \bar{\psi} \not{\partial} \psi + \frac{N}{J_K} \bar{\psi} \psi \\ & + b \bar{\psi} \psi + b \bar{\psi} \psi + \frac{N}{J_K} \bar{\psi} \psi \\ & + \frac{N}{2e^2} (\not{\partial} \psi)^2 + N g j (\not{\partial} + i a) \bar{\psi} \psi + \end{aligned} \quad (61)$$

where L_E is a shorthand for L_E^* with $\gamma = 1$. The last two terms are two examples of the terms that will be generated in the coarse graining process. They are written on the grounds of gauge invariance. In Sec. VI we show that these new terms and other terms grouped in the ellipsis are irrelevant at our finite coupling Kondo transition fixed point. Embedded in Eq. (61), is the QED₃ Lagrangian density

$$\bar{\psi} \not{\partial} \psi + \frac{N}{2e^2} (\not{\partial} \psi)^2 + \quad (62)$$

QED₃ has been studied before as the low-energy theory of the staggered flux phase^{12,14}. We have used the recent result¹³ about the irrelevance of instanton events near the QED₃ fixed point and took the gauge eld to be non-compact. In our formulation the physical SU(2) theory corresponds to $N = 2$ four-component spinors. It could have been formulated as $N_f = 4$ two-component spinors near each node in the Brillouin zone. To go back and forth between these formulations one just needs to use $N_f = 2N$.

IV. 1/N SYSTEMATIC EXPANSION: FIELD PROPAGATORS

The Lagrangian density Eq. (61), derived in the previous section, allows us to develop the machinery of 1/N expansion. The propagators for the elds b and a are of

order 1/N in the large N limit. This will allow us to calculate different propagators and scaling dimensions order by order in 1/N.

We start with our notations for propagators of the fermion elds, and $\bar{\psi}$. We use a single line notation for the eld propagator and a double line for propagator:

$$\bar{\psi}_i^a \psi_j^b(q) = i \overleftrightarrow{\text{---}}^q \text{---} j = \bar{\psi}_i^a i \overleftrightarrow{\text{---}}^q j^b; \quad (63)$$

$$\bar{\psi}_i^a \psi_j^b(q) = i \text{---}^q \text{---} j = \bar{\psi}_i^a i \text{---}^q j^b; \quad (64)$$

where Feynman's slash notation

$$\not{q} = \gamma_\mu q_\mu \quad (65)$$

is used.

The Gauge Field a . Our Lagrangian density L_E has a QED₃ piece

$$\bar{\psi} \not{\partial} \psi + \frac{N}{2e^2} (\not{\partial} \psi)^2 + \quad (66)$$

which has been studied before.^{12,16} We refer the reader to the Appendix B of Ref. 14 for the calculation of the QED₃ gauge propagator. The QED₃ gauge propagator, in the leading order, is given by:

$$h a_i(q) = \text{---}^q \text{---} = \frac{8}{N j j} + \frac{q q}{q^2} (1); \quad (67)$$

where ξ is the Fadeev-Popov gauge fixing parameter. $\xi = 1$ corresponds to the Feynman gauge and $\xi = 0$ to the Landau gauge. The $j j$ dependence comes from calculating the self energy

$$\text{---}^k \text{---}^q \text{---}^k : \quad (68)$$

The charge e has disappeared from the final result. This charge appears if one includes the q^2 dependence in the denominator of the gauge propagator. But in the small q (long distance) limit, the $j j$ dependence dominates over q^2 term, no matter how large e is. Another way to say this is that the QED₃ is self-critical. It will flow to a stable fixed point even if we start with a large gauge charge e at least for some large N .

The gauge propagator of our theory, in the leading order, will come solely from the f -fermion bubble, given diagrammatically in Eq. (68). The b propagation does not contribute to the gauge eld's self energy in the

leading order. Therefore, in the leading order, $\hbar b i^{-1}(q)$ of our Lagrangian density Eq. (61) is the same as QED₃.

The Kondo Field b . The b field propagator, in the leading order, is given by:

$$\hbar b i^{-1}(q) = G_b^{-1}(q) = G_{b0}^{-1}(q) \text{ (diagram: a circle with two arrows, one labeled } k \text{ and the other } k+q \text{)}; \quad (69)$$

where $G_{b0}^{-1}(q) = N=J_K + O(q^2)$. The self energy is easily obtained to be:

$$\begin{aligned} \text{(diagram: a circle with two arrows, one labeled } k \text{ and the other } k+q \text{)} &= (ij)N \frac{d^d k}{(2\pi)^d} \text{Tr} \frac{1}{k} \frac{1}{k+q} \\ &= \frac{N}{4} \frac{1}{ij} + \frac{2N}{2} \end{aligned} \quad (70)$$

This will result in the following b propagator:

$$\hbar b i(q) = \text{(diagram: a double-dashed line with an arrow labeled } q \text{)} = \frac{4}{N(jj + m_b)}; \quad (71)$$

where m_b is the effective mass of the b propagator, and is given by:

$$m_b = \frac{4}{J_K} - \frac{8}{2} / (J_K^{cr} - J_K); \quad (72)$$

where J_K^{cr} is given by $J_K^{cr} = \frac{2}{2} = 2$. J_K^{cr} is of course nonuniversal, i.e. it depends on how we regularize the integral in Eq. (70). However the final result that

$$m_b / (J_K^{cr} - J_K) \quad (73)$$

is scheme independent.

The above result, that the mass of the b field can be tuned to zero, serves as a sanity check for the mean-field result of the finite coupling Kondo transition obtained in Sec. II A.

Since the self energy has jj dependence, in the long distance (small jj) limit, it dominates over the q^2 dependence coming from $j b j$. The q^2 dependence is ignored in the final expression given in Eq. (71). In the RG language, the $j b j$ term is irrelevant at the fixed point.

We also mention a further notation for the massless b propagator. We have used the "double-dashed" line notation for b propagator away from the critical point. We use a "single-dashed" line for the b propagator at the critical point:

$$\text{(diagram: a single-dashed line with an arrow labeled } q \text{)} = \frac{4}{N jj}; \quad (74)$$

Except for the calculation of b , done in Sec. V A 1, massless b propagator of Eq. (74) is used throughout the paper.

The b propagator given by Eqs. (71) and (74) is gauge invariant. This will not be the case to all orders in perturbation theory. The reason is as follows. There is a gauge freedom in defining b . Given that the action is gauge invariant, the interaction $b^a a + b^a a^a$ dictates that gauge transformation

$$b(x) \rightarrow e^{i\alpha(x)} b(x) \quad (75)$$

has to be accompanied by

$$b(x) \rightarrow e^{i\alpha(x)} b(x); \quad (76)$$

since b can not tolerate any gauge freedom. So the b propagator in principle should have a gauge dependence. However to leading order, the gauge field propagator does not enter in b 's self energy and that is why the leading order b propagator given by Eq. (71) is gauge invariant.

V. CRITICAL PROPERTIES OF THE FIXED POINT

A. Divergence of The Correlation Length: the Exponent

In this section we go through the calculation of the divergence of the correlation length near the fixed point by calculating the exponent:

$$1 / \frac{1}{jj - J_K^{cr}}; \quad (77)$$

We mention first what the correlation length means by looking at the Kondo (Heisenberg) Hamiltonian in different regimes. At $J_K = 0$ the Kondo (Heisenberg) Hamiltonian has two decoupled parts: the kinetic term for the conduction electrons and the anti-ferromagnetic Heisenberg exchange of the localized spins. There is no entanglement between conduction electrons and the localized spins in the ground state. In the large J_K limit the Kondo term dominates over the Heisenberg exchange. The ground state is the product of conduction electrons and the localized spin singlets at each site. Since we are at half filling every conduction electron is taken away by a localized spin. There is entanglement in the ground state. But the entanglement is restricted to one site. As we approach the critical point, the "size" of these Kondo singlets grows and it eventually diverges at the critical point. The scale associated with these Kondo singlets is what we mean by the correlation length.

The relevant flow of the mass term $j b j$ will introduce a diverging length scale ξ_b near the transition point. Since the Kondo phase is characterized by the condensation of the b field, the correlation length is proportional to ξ_b . This results in

$$\xi_b = \xi_b; \quad (78)$$

We obtain γ_b by using the scaling relation²⁰

$$\gamma_b = \frac{\gamma_b}{2}; \quad (79)$$

where γ_b and $2 - \gamma_b$ characterize the power-law behavior of two-point function $G_b(k; m_b)$

$$\langle b(x) b(x^0) \rangle = \int \frac{d^3 k}{(2\pi)^3} e^{ik \cdot (x - x^0)} G_b(k; m_b) \quad (80)$$

in two different limits:

$$G_b(0; m_b \rightarrow 0) \sim m_b^{-\gamma_b}; \quad (81)$$

$$G_b(k \rightarrow 0; 0) \sim |k|^{2-\gamma_b}; \quad (82)$$

It should be noted that since b is not gauge invariant, γ_b and γ_b are not gauge invariant. However by definition, given by Eq. (77), is a gauge invariant quantity. Since it is not a priori obvious that the scaling relation given by Eq. (79) is gauge invariant, we calculate γ_b and γ_b in a general gauge, and show that derived from Eq. (79) is indeed gauge invariant.

The methods we use to calculate γ_b and γ_b are very different. The calculation of γ_b is done by directly calculating the Green's function $G_b(0; m_b)$. Calculating γ_b , in this manner, is much more involved. Instead, we calculate γ_b by relating γ_b to the scaling dimension of $\bar{\psi}\psi$. The scaling dimension of $\bar{\psi}\psi$ is then obtained by perturbing the Lagrangian density $\mathcal{L}_E \rightarrow \mathcal{L}_E + \bar{\psi}\psi$ and applying the Callan-Symanzik equation for the propagator $\bar{\psi}\psi$, in the presence of the perturbation, to obtain the flow of the composite operator $\bar{\psi}\psi$, and thus extracting its scaling dimension.

1. γ_b

To calculate γ_b we calculate $G_b(0; m_b)$, i.e. the uniform part of the b propagator slightly away from the critical point. From the calculations in the previous section leading to Eq. (71) we have

$$G_b^{-1}(0; m_b) = N \frac{m_b}{4} G_b^{1=N}(0; m_b); \quad (83)$$

where $G_b^{1=N}(0; m_b)$ is given diagrammatically by

$$\begin{aligned} G_b^{1=N}(0; m_b) = & \text{Diagram 1} + \text{Diagram 2} + \text{Diagram 3} + \text{Diagram 4} \\ & = -\frac{1}{2} m_b \log(m_b) : \end{aligned} \quad (84)$$

This results in

$$\begin{aligned} G_b^{-1}(0; m_b) = N \frac{m_b}{4} \left[1 - \frac{4}{N} \left(\frac{1}{2} \right) \log(m_b) \right] \\ \sim m_b^{1 - \frac{4}{2N}}; \end{aligned} \quad (85)$$

from which we obtain

$$\gamma_b = 1 - \frac{4}{2N}; \quad (86)$$

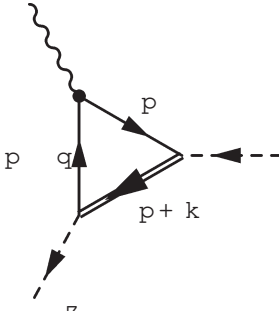
The integrals are evaluated in the dimensional regularization scheme.^{23,25} The mass scale in this scheme is introduced to keep track of dimensions in d dimensional integration and plays the role of a UV cutoff. A simple pole in the dimension d reflects the logarithmic divergence of the original 3 dimensional integration. We only keep track of the IR divergent parts. As far as the universal properties of the fixed point are concerned this regularization would give the same answer as a cutoff regularization.

We briefly discuss the diagrams involved in $G_b^{1=N}(0; m_b)$. The first diagram of Eq. (84) has no m_b dependence. The second and third diagrams are equal and are given by:

$$\text{Diagram 2} = \frac{1}{2} m_b \log(m_b) : \quad (87)$$

The last diagram of Eq. (84) contains the vertex that

couples b bosons with the gauge field:

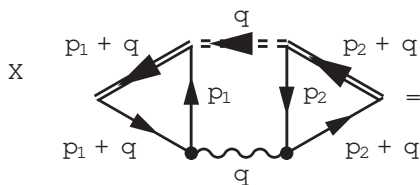


$$= +N \frac{d^3 p}{(2\pi)^3} \text{Tr} \left[\not{p} + \not{k} \not{p}^{-1} \not{p} \not{q}^{-1} \right] : \quad (88)$$

In the calculation of $\Gamma_b^{(1=N)}(0; m)$ the momentum entering this vertex is zero. The result of this integral for $k = 0$ is

$$\int \frac{d^3 p}{(2\pi)^3} \text{Tr} \left[\not{p}^{-1} \not{p}^{-1} \not{p} \not{q}^{-1} \right] = \frac{q}{4\pi j} : \quad (89)$$

Having the result of the above integral, we get



$$= -\frac{1}{2} m_b \log(m_b) : \quad (90)$$

2. b

b is easily related to the scaling dimension of the field at the critical point [See Eq. (82)] :

$$b = 1 + 2[b] : \quad (91)$$

Since the only way for the field to propagate is to decay into $a a$, the scaling of the self energy of b is the same as the propagator of the composite operator $a a$. This observation results in

$$[b] = 3 - [a a] : \quad (92)$$

Thus b is known once we know the scaling dimension of the composite operator $a a$.

The scaling dimension of $a a$ is obtained by adding the perturbation

$$L_E \rightarrow L_E + \int a a \quad (93)$$

to the Lagrangian density and obtaining the flow of b by studying the Callan-Symanzik equation for the propagator $\langle a(x) a(x^0) \rangle$.

The Callan-Symanzik equation is essentially the "scale invariance" relation.^{23,24} Near the fixed point, a change in scale has to be accompanied by the flow of some coupling constants and scaling of the fields to maintain scale

invariance. For the propagator under consideration it will read

$$\frac{\partial}{\partial \lambda} \langle a a \rangle + \frac{dC_m}{d\lambda} \frac{\partial}{\partial C_m} \langle a a \rangle = 0; \quad (94)$$

where λ and C_m are scaling dimensions of the fields and m . The set C includes the coupling constants that flow. For the perturbation given by Eq. (93) it has only 1 element:²⁸

$$C = \int a a : \quad (95)$$

It is more convenient to apply the Callan-Symanzik equation to the momentum-space Green's function $\langle a a \rangle(k)$

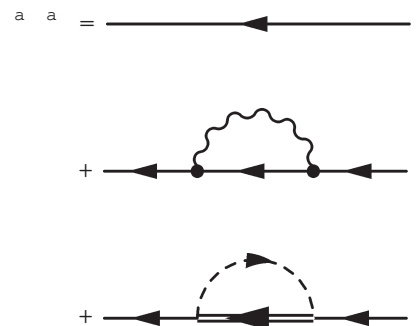
$$\langle a a \rangle(k) = \int \frac{d^3 k}{(2\pi)^3} e^{ik(x-x^0)} \langle a(x) a(x^0) \rangle : \quad (96)$$

Eq. (94) results in

$$\frac{\partial}{\partial \lambda} \langle a a \rangle + (3 - [a a]) \frac{d}{d\lambda} \langle a a \rangle = 0; \quad (97)$$

where "3" is coming from the scaling of the measure $d^3 k$ in the integrand of Eq. (96).

To apply the Callan-Symanzik equation we first need to obtain $[a a]$ and $\frac{d}{d\lambda}$. The gauge dependant $[a a]$ is obtained by calculating the propagator



$$+ \dots : \quad (98)$$

The result is

$$\langle a a \rangle(k) = (ik)^{-1} \left(1 + \frac{1}{N} \left(\frac{2}{2} + \frac{4}{2} \right) (1 - [a a]) \log(jk) \right); \quad (99)$$

from which we get

$$[a a] = 1 + \frac{1}{N} \left(\frac{1}{2} + \frac{2}{2} \right) (1 - [a a]) : \quad (100)$$

Similarly, calculating the gauge invariant conduction

electron propagator

$$\begin{aligned}
 a \rightarrow a &= \text{diagram with two parallel lines and a right-pointing arrow} \\
 &+ \text{diagram with two parallel lines, a dashed arc above, and two right-pointing arrows} \\
 &= (i\epsilon)^{-1} \left[1 + \frac{2}{3^2 N} \log(jk) \right]
 \end{aligned} \quad (101)$$

results in the gauge invariant

$$= 1 + \frac{1}{3^2 N} : \quad (102)$$

The logarithmic infrared divergence of Eq. (101) can be interpreted as the scaling of the quasi-particle weight Z , defined by $a \rightarrow a(k) = Z (i\epsilon)^{-1}$. The scaling form of Z which is consistent with Eq. (101) is

$$Z = \frac{k}{j^2} \frac{1}{j^2 N} : \quad (103)$$

The vanishing of the Z factor as $k \rightarrow 0$ can in principle be seen in tunnelling experiments. This non-Fermi liquid behavior arises, because at the Kosterlitz-Thouless fixed point, there are very strong scattering of conduction electrons into the fermions. This is due to the fact that the boson field which causes the scattering has become massless.

The next step is to obtain $a \rightarrow a(k)$ in the presence of the perturbation $a \rightarrow a$ given by Eq. (93). This perturbation is represented diagrammatically by

$$\text{diagram with two parallel lines and a star} = : \quad (104)$$

The diagrammatic expression for $a \rightarrow a$ is then given

by

$$\begin{aligned}
 a \rightarrow a &= \text{diagram with two parallel lines and a star} \\
 &+ \text{diagram with two parallel lines, a star, a wavy line, and two right-pointing arrows} \\
 &+ \text{diagram with two parallel lines, a star, a dashed arc above, and two right-pointing arrows} \\
 &+ \text{diagram with two parallel lines, a dashed arc above, a star, and two right-pointing arrows} \\
 &+ \text{diagram with two parallel lines, a star, a dashed arc above, and two right-pointing arrows} \\
 &+ \text{diagram with two parallel lines, a star, a dashed arc above, and two right-pointing arrows}
 \end{aligned} \quad (105)$$

It results in

$$a \rightarrow a(k) = (i\epsilon)^{-2} \left[1 + \frac{4}{3^2 N} \log(jk) \right] : \quad (106)$$

Callan-Symanzik equation [Eq. (97)] applied to the above propagator results in

$$\frac{d}{dl} = 1 + \frac{8}{3^2 N} + \frac{2}{2N} (1) : \quad (107)$$

The above relation together with Eq. (92) yields:

$$b = 1 + \frac{1}{N} \left[\frac{8}{3^2} + \frac{2}{2} (1) \right] : \quad (108)$$

Combine this with Eq. (91) to get

$$b = 1 + \frac{1}{N} \left[\frac{16}{3^2} + \frac{4}{2} (1) \right] : \quad (109)$$

Collecting what we have obtained for b and b given by Eqs. (86) and (109), together with the scaling relation given by Eq. (79), we arrive at the gauge invariant

$$= 1 + \frac{16}{3^2 N} : \quad (110)$$

Note that the $1=N$ fluctuations have brought us further away from the generic $1=2+O(\epsilon)$ result one would obtain for a stable fixed point in an expansion (which is an expansion around the gaussian action), assuming there exists such a stable fixed point.

B. Staggered Spin Correlation

We continue the study of the physical properties of our K I{ASL fixed point by obtaining staggered spin $M = S_A - S_B$ correlation at the fixed point. The correlation is algebraic and our fixed point is an algebraic spin liquid fixed point.

Since the decay exponent of $hM(x) = M(x)$ and $hM^+(x)M^-(x)$ is the same, it suffices to find the scaling dimension of M^+ . In terms of the field operators $M^+(x)$ is

$$M^+(x) = \frac{1}{2} (M_1(x) - M_2(x)); \quad (111)$$

where M is a 4×4 matrix, which should be obtained from the relation between the field and the microscopic operators developed in Sec. III. Physically 1 and 2 represents \uparrow and \downarrow . In $1=N$ expansion they are 2 indices among many. M is obtained to be²⁹

$$M = \frac{1}{2} \begin{pmatrix} 1 & 0 & 0 & 0 \\ 0 & 1 & 0 & 0 \\ 0 & 0 & 1 & 0 \\ 0 & 0 & 0 & 1 \end{pmatrix}; \quad (112)$$

We should add this perturbation to the Lagrangian and study its flow. However $\frac{1}{2} (M_1(x) - M_2(x))$ mixes with $\frac{1}{2} (M_1(x) + M_2(x))$. In other words M^+ is not a scaling operator. Having this in mind, we perturb the Lagrangian density by

$$L_E = U_+ \frac{1}{2} (M_1(x) - M_2(x))^2 + u_+ \frac{1}{2} (M_1(x) + M_2(x))^2 \quad (113)$$

and study the Callan-Symanzik equation for the propagators $\frac{1}{2} \langle M_1^2(k) \rangle$ and $\frac{1}{2} \langle M_2^2(k) \rangle$. The result (obtained in Appendix B) is

$$\frac{\partial}{\partial \Lambda} \left(\frac{1}{2} \langle M_1^2(k) \rangle \right) = \frac{1}{2} \left(\frac{2}{N} \right) \left(\frac{1}{2} \langle M_1^2(k) \rangle \right) + \frac{1}{2} \left(\frac{2}{N} \right) \left(\frac{1}{2} \langle M_2^2(k) \rangle \right); \quad (114)$$

We emphasize that off-diagonal terms make $1=N$ correction to the scaling dimension of the staggered spin. This is because the scaling dimensions of \uparrow and \downarrow are equal in the infinite N limit. This is similar to the importance of off-diagonal terms in the 1st order degenerate perturbation theory in quantum mechanics.

The largest eigenvalue $1 + \frac{2}{3} \frac{1}{N} = (3/2N)$ of above matrix dominates the scaling of M^+ . The dominant scaling dimension of M^+ , denoted by $[M^+]$, is then given by

$$[M^+] = 2 - \frac{2}{3} \frac{1}{N} = \frac{31}{3} \frac{1}{N}; \quad (115)$$

The decay exponent of the correlation function results immediately:

$$hM(x) = M(x) / \frac{1}{x^{0.5[M^+]}} + \dots; \quad (116)$$

where the ellipsis denotes the decay with the larger exponent coming from the other eigenvalue of the matrix in Eq. (114).

Finally, we mention a comparison between our result and the Rantner-Wen studies.¹² They studied spin correlations in their large- N QED₃ effective field theory in the Landau gauge. They were interested in the similar bilinear form as we have here with $M = 1$. In our calculation any bilinear form with the property $[M;] = 0$ has the same scaling dimension. To check our result we turned off all contributions to the exponent coming from terms involving ψ . The result $[M^+]_{\text{ASL}} = 2/32 = (3/2N)$ obtained in Feynman gauge agrees with theirs obtained in Landau gauge. $2[M^+]_{\text{ASL}}$ corresponds to the decay exponent of localized spin correlation when we are in the ASL phase, where the Kondo field is massive. As expected, we have $[M^+]_{\text{ASL}} < [M^+]$, i.e. the Neel fluctuations are stronger in the ASL phase than at the K I transition, where the Kondo singlets are forming.

In the $J < J_K^{\text{cr}}$ regime the ASL is in the presence of the semimetal (described by field) and the gapped Kondo field. The question may arise whether the semimetal would destabilize the ASL. The semimetal will not destabilize the ASL, because integrating out ψ and b fields in this phase will produce (retarded) four-fermion interaction term among fields. These four-fermion interactions are irrelevant at the ASL fixed point.

V I. STABILITY OF THE FIXED POINT

In this section we discuss the issue of the stability of the K I{ASL fixed point in the honeycomb lattice to 1st order in $1=N$. There are two separate issues one has to consider in the stability of this fixed point.

In going to the continuum limit we have dropped the compact character of the gauge field. This is only justified if the instanton events, where the flux of the gauge field suddenly changes by 2π , do not proliferate. For $J_K > J_K^{\text{cr}}$ the Kondo field b is condensed and we are in the Higgs phase. Gauge field is massive, its fluctuations are suppressed and instantons do not proliferate. Addressing the proliferation of instantons in the regime where the Kondo phase has disappeared is more subtle. We know from Polyakov's work that the compact pure gauge theory in $2+1$ dimension is in the confining phase for all coupling constant, i.e. for all coupling constants the instantons proliferate.²¹ It has been argued recently that coupling the gauge field to massless Dirac fields results in a deconfined phase for sufficiently large N .¹³ This is due to the fact that the massless matter field, in this case Dirac fields, suppress the fluctuations of the gauge field. We apply that argument here and assume that the

gauge field in the $J_K < J_K^{cr}$ regime is in a deconfined phase. At the K I {ASL} fixed point, due to the presence of an extra massless matter field, i.e. the Kondo field b , the gauge field fluctuations are suppressed even more.

Next we focus on the instanton (free) sector. At the fixed point the gauge field a , boson b and two fermion fields $\psi, \bar{\psi}$; all have scaling dimension $1 + O(1/N)$. This can be seen by the form of propagators derived in Sec. IV. The large N scaling dimension of a , b , and ψ will limit our choices for relevant perturbations. Different such perturbations are discussed below:

b mass term: this term is already present in the microscopic bare Lagrangian. We have to tune J_K to make the effective mass of the b field to be zero. This perturbation is indeed relevant.

a mass terms: these mass terms either break the $SU(N)$ flavor symmetry or the particle-hole and rotation symmetry.

b kinetic term of the form $b(\partial + ia)b$: this term violates the particle-hole symmetry. It has to be accompanied by $b(\partial - ia)b$ with an equal coefficient. But $b\partial b + b\partial b = \partial(bb)$ is a total derivative.

b kinetic term of the form $L = N g j(\partial + ia)b^\dagger$: this term is irrelevant by the power counting. That is

$$\frac{dg}{dl} = -1 + O(1/N)g;$$

Kinetic terms for ψ and $\bar{\psi}$ fields: these are the only potentially dangerous perturbations, because they are marginal in the $N \rightarrow 1$ limit. Actually in the derivation of the Lagrangian density Eq. (61) we set $v_c = v_f$ to make the action Lorentz invariant. We have to consider perturbations that break this "tuned" Lorentz symmetry and study their flow. By scaling argument the flow of these perturbations is marginal to first order in $1/N$: marginally irrelevant, relevant, or exactly marginal. Our calculations results in the marginal irrelevance of these types of perturbations. We discuss this issue below.

We break the Lorentz symmetry by adding the perturbation

$$L_E^a = \sum_{\mathbf{r}} \psi^\dagger(\mathbf{r}) \psi(\mathbf{r}) + \frac{1}{2} \sum_{\mathbf{r}} \psi^\dagger(\mathbf{r}) \psi(\mathbf{r}) (\partial + ia) \psi(\mathbf{r})$$

to the Lagrangian density. The perturbation has to be considered both in ψ and $\bar{\psi}$ fields because of their mixing due to the exchange of the b field. Applying Callan-Symanzik equation to the propagators

and $\psi^\dagger \psi$ results in the following RG flow:

$$\frac{d}{dl} \begin{pmatrix} \langle \psi^\dagger \psi \rangle \\ \langle \psi^\dagger \psi \rangle \\ \langle \psi^\dagger \psi \rangle \\ \langle \psi^\dagger \psi \rangle \end{pmatrix} = D \begin{pmatrix} \langle \psi^\dagger \psi \rangle \\ \langle \psi^\dagger \psi \rangle \\ \langle \psi^\dagger \psi \rangle \\ \langle \psi^\dagger \psi \rangle \end{pmatrix}; \quad (117)$$

where the matrix anomalous dimension D is given by

$$D = \frac{1}{15 - 2N} \begin{pmatrix} 2 & 74 & 32 & 32 & 2 & 4 & 3 \\ 6 & 32 & 74 & 32 & 4 & 2 & 4 \\ 32 & 32 & 74 & 4 & 4 & 4 & 2 \\ 4 & 2 & 4 & 10 & 0 & 0 & 0 \\ 4 & 4 & 2 & 0 & 0 & 0 & 10 \end{pmatrix}; \quad (118)$$

Eigenvalues of this matrix anomalous dimension are all negative except for one trivial zero eigenvalue. The zero eigenvalue is trivial since the corresponding perturbation can be absorbed by scaling ψ and $\bar{\psi}$ fields, shown in Appendix A.

We knew from the mean-field result that there exist a fixed point in the parameter space. But our results goes further by ruling out a multicritical fixed point. So based on our result, for large enough N , this quantum critical point will be achieved by tuning one parameter J_K .

VII. CONCLUSIONS

We have studied the Kondo-Hubbard model on the honeycomb lattice at half filling. The main motivation for our study is that the Kondo band gap vanishes at a finite Kondo coupling constant (even as $J_H \rightarrow 0$) so that a novel kind of quantum phase transition becomes possible.

In this paper we considered the transition of this Kondo insulator (KI) to a spin liquid phase which is later identified to be algebraic spin liquid (ASL). We developed a mean-field theory for such a transition using a fermionic representation for spins. To consider fluctuations about this mean-field systematically, we adopted a large N generalization of our model by having N spin-flavors rather than just f^\uparrow, f^\downarrow . We found that the KI {ASL} transition is controlled by a stable Lorentz invariant fixed point.

In the KI phase, the Kondo field b condenses and we are in the Higgs phase where the gauge field is massive. ASL phase is described by "decoupled" QED₃ (coming from $J_H S_i \cdot S_j$ interaction) and the Dirac conduction electrons. They are "decoupled" in that the Kondo field that couples these two terms is now massive. The gauge field is deconfined in the ASL.

We were able to calculate the exponent $\nu = 1 + 16/(3 - 2N)$ of the diverging length scale near the transition. Interestingly, $1/N$ fluctuations have pushed the infinite N result further away from the result $\nu = 1/2$

one would get from the Landau-type expansion. We noted that at our fixed point the quasi-particle weight of the conduction electron vanishes which is indicative of non-Fermi liquid behavior. We also calculated the decay exponent of the staggered spin $M = S_A - S_B$ correlation at the fixed point. This is not a scaling operator, since it mixes with $m = S_A + S_B$. The dominant decay exponent turned out to be $2[M + \frac{1}{2}] = 4 - \frac{4}{7 + \sqrt{73}} = (3^2 N)^{-4/622} = (3^2 N)^{-1/155.5}$. On the other hand, in the ASL phase M is a scaling operator with the decay exponent $2[M + \frac{1}{2}]_{\text{ASL}} = 4 - \frac{4}{64} = (3^2 N)^{-1/16}$. The jump in this exponent, as one gets to the KI transition point, is due to the fact that there exists an extra massless matter field at the transition (in this case Kondo field b), which modifies the exponent. This jump and its significance was discussed in a different context recently.¹⁸

The quantum phase transition between the KI and ASL does not break any physical symmetry. The KI{ASL transition is essentially a Higgs(deconfinement) transition. In other words, what changes at the transition point is the dynamics of the gauge field. This by itself is an interesting property of the transition we have studied, which is realized in a minimal Kondo{Heisenberg model.

In connection to this work, we are currently pursuing the numerical study of this model; using a quantum Monte Carlo technique without the fermion sign problem.

VIII. ACKNOWLEDGMENTS

We thank Michael Hermele for many insightful comments and suggestions and we thank T. Senthil and X.-G. Wen for helpful discussions. P. A. L. acknowledges the support by the Department of Energy under grant DE-FG 02-03ER 46076.

APPENDIX A: RESTORATION OF THE LORENTZ INVARIANCE

Here we will give more details regarding the irrelevance of the perturbations that break the Lorentz symmetry at our Lorentz invariant KI{ASL fixed point. It is tempting to break the Lorentz invariance by perturbing only one field, or b . However a and b lose their own identity as b becomes massless and they mix together. Having this mixing in mind we consider the most general perturbation which is of the kinetic form for the a and b fields, and is consistent with the gauge symmetry

$$L_E^a = \sum_a \int d^3x \left[\frac{1}{2} (\partial_\mu a)^2 + \frac{1}{2} (\partial_\mu b)^2 + \frac{1}{2} (\partial_\mu a + \partial_\mu b)^2 \right] \quad (A1)$$

The corrections to fermion propagators and gauge vortex is represented diagrammatically:

$$\begin{aligned} \text{Diagram 1: } \text{Feynman diagram with two external fermion lines (double lines) and a central circle loop.} &= i \epsilon; \\ \text{Diagram 2: } \text{Feynman diagram with two external fermion lines (single lines) and a central square loop.} &= i \epsilon; \\ \text{Diagram 3: } \text{Feynman diagram with two external fermion lines (single lines) and a central square loop with a wavy line attached to the top.} &= +i \epsilon; \end{aligned} \quad (A2)$$

where we have used the notation

$$\epsilon = \frac{1}{2} \int d^3x \left[(\partial_\mu a)^2 + (\partial_\mu b)^2 \right] \quad (A3)$$

We evaluate the two propagators $\langle a a \rangle$ and $\langle a b \rangle$ in the presence of the perturbation given by Eq. (A1).

We obtain

$$\begin{aligned} \alpha_a(k) = & \frac{1}{k} \left(1 + \frac{2}{2N} \log(kj) \right) \\ & + i \frac{1}{k} \frac{1}{k} \frac{1}{k} + \frac{\log(kj)}{15 \cdot 2N} j \quad jF; \quad ; \end{aligned} \quad (A.9)$$

where F_j is given by

$$F_j = 104 \quad 32 \quad 32 + 2 + 4 + 4 : (A.10)$$

From Eq. (A.9), we obtain the scaling dimension of the field in Feynman gauge :

$$= 1 + \frac{1}{2N} : (A.11)$$

Then we use the Callan-Symanzik equation machinery by scaling the momentum $k \rightarrow ek$ and applying

$$\frac{\partial}{\partial \lambda} + (3 - 2) + \frac{dC_m}{d\lambda} \frac{\partial}{\partial C_m} \alpha_a = 0; (A.12)$$

$$\frac{\partial}{\partial \lambda} + (3 - 2) + \frac{dC_m}{d\lambda} \frac{\partial}{\partial C_m} \alpha_a = 0; (A.13)$$

where the set C includes the coupling constants that flow. For the perturbation under consideration it has 6 elements:

$$C = f_0; i_1; i_2; o_1; i_2; g;$$

Eqs. (A.12), and (A.13) will lead to the RG flow :

$$\frac{\partial}{\partial \lambda} \begin{pmatrix} 6 \\ 6 \\ 6 \\ 6 \\ 4 \end{pmatrix} = D \begin{pmatrix} 6 \\ 6 \\ 6 \\ 6 \\ 4 \end{pmatrix}; \quad (A.14)$$

where the matrix anomalous dimension D is given by

$$D = \frac{1}{15 \cdot 2N} \begin{pmatrix} 74 & 32 & 32 & 2 & 4 & 3 \\ 32 & 74 & 32 & 4 & 2 & 2 \\ 32 & 32 & 74 & 4 & 4 & 2 \\ 2 & 4 & 4 & 10 & 0 & 0 \\ 4 & 2 & 4 & 0 & 10 & 0 \\ 4 & 4 & 2 & 0 & 0 & 10 \end{pmatrix} : (A.15)$$

All the eigenvalues of this matrix anomalous dimension is nonpositive. There is one zero eigenvalue with the corresponding eigenvector

$$\begin{pmatrix} 2 \\ 6 \\ 6 \\ 6 \\ 6 \\ 4 \end{pmatrix} \begin{pmatrix} 3 \\ 7 \\ 7 \\ 7 \\ 7 \\ 5 \end{pmatrix} :$$

The above shift can be absorbed by scaling fields separately. The scaling is delicate, since in our RG scheme we have fixed the coefficient of $b^a a + c$ to be 1. So the scaling of a and b has to be accompanied by an appropriate scaling of c . But this - in general - will move us away from the critical point. For the above perturbation though, the scaling factor for b is 1:

$$\frac{1}{1 + \frac{1}{15 \cdot 2N}} = 1 + O(\frac{1}{N^2}) :$$

So the above perturbation remains exactly marginal to all orders in $1/N$.

It is interesting to note that the uniform shift

$$\begin{pmatrix} 2 \\ 6 \\ 6 \\ 6 \\ 6 \\ 4 \end{pmatrix} \begin{pmatrix} 3 \\ 7 \\ 7 \\ 7 \\ 7 \\ 5 \end{pmatrix}$$

is an eigenvector with a negative eigenvalue. Why should this perturbation flow? The absorption of the uniform perturbation in a and b has to be accompanied by scaling the b field by

$$\frac{1}{1 + \frac{1}{15 \cdot 2N}} = 1 + O(\frac{1}{N^2}) : (A.16)$$

This scaling of the b field will move us away from the critical point.

APPENDIX B: STAGGERED SPIN CORRELATION

In this appendix we will find the algebraic decay exponent of $\langle M(x) M(y) \rangle$ at K1/ASL fixed point. We do this by obtaining the staggered spin M scaling dimension. It suffices to find the scaling dimension of M^+ , since the decay exponent of $\langle M(x) M(y) \rangle$ and $\langle M^+(x) M^-(y) \rangle$ is the same. The first step is to translate M^+ to the field theory language with the dictionary provided by Eq. 53. The expanded form is given by

$$\begin{pmatrix} 2 \\ 6 \\ 6 \\ 6 \\ 4 \end{pmatrix} \begin{pmatrix} f_{A+} \\ f_{B+} \\ f_{B-} \\ f_{A-} \\ i \end{pmatrix} \quad (B.1)$$

$$= \begin{pmatrix} h \\ f_{A+}^y \\ f_{B+}^y \\ f_{B-}^y \\ f_{A-}^y \end{pmatrix} \begin{pmatrix} i \\ i \\ i \\ i \\ i \end{pmatrix} \quad (B.2)$$

Start with the expression for $S_A^+ = S_A^1 + iS_A^2 = f_A^{1y} f_A^2$, which leads to

$$S_A^+(x) = \begin{pmatrix} 0 & 1 \\ 1 & 0 \end{pmatrix} \begin{pmatrix} B \\ C \end{pmatrix} \begin{pmatrix} 0 \\ 2 \end{pmatrix} (x) : \quad (B.3)$$

